Supporting information for "A theoretical and empirical assessment of stomatal optimization modeling" by Yujie Wang, John S. Sperry, William R.L. Anderegg, Martin D. Venturas, and Anna T. Trugman

Article acceptance date: 9 March 2020

Notes S1 Marginal water use efficiency when $E_{leaf} = 0$

Marginal water use efficiency must be higher than the marginal risk when $E_{leaf} = 0$ for the two functions intersect. When $E_{leaf} = 0$, the net assimilation rate is 0 during the day. With an incremental increase in E_{leaf} to ∂E, the leaf diffusive conductance for CO_2 increases by $\partial G = \partial E / (1.6 \times D)$ (in mol CO_2 m^{-2} s^{-1}) neglecting the leaf termperature change, where D is the leaf-to-air vapor pressure deficit relative to atmospheric pressure. The net photosynthesis increases by ∂A:

$$\partial A = \partial G \cdot (C_a - C_i) - G \cdot \partial C_i = \frac{\partial E}{1.6 \cdot D} \cdot (C_a - C_i) - \frac{E}{1.6 \cdot D} \cdot \partial C_i \,, \quad \text{S1.1}$$

where C_a is the atmospheric CO_2 concentration in μmol mol^{-1}, and C_i is the intercellular CO_2 concentration. The ∂A is maximal when $E_{leaf} = 0$ because $C_a - C_i$ is maximal and $\frac{E}{1.6 \cdot D} \cdot \partial C_i = 0$. As ∂E is infinitesimal, $C_a - C_i \approx C_a - \Gamma$, where Γ is the CO_2 compensation point with the presence of dark respiration. Thus, the marginal water use efficiency when $E_{leaf} = 0$ is given as:

$$\frac{\partial A}{\partial E}\Big|_{E_{leaf}=0} = \frac{C_a - \Gamma}{1.6 \cdot D}. \quad \text{S1.2}$$

The unit for $\partial A/\partial E$ is μmol CO_2 mol^{-1} H_2O.

Equations S1.1 and S1.2 provide a quick estimation of $\partial A/\partial E$ when $E_{leaf} = 0$. For the case when $E_{leaf} > 0$, neglecting the leaf cooling caused by transpiration, the $\partial A/\partial E$ can be derived as following. As $A = G \cdot (C_a - C_i)$, $\partial A/\partial G$ can be computed using:

$$\frac{\partial A}{\partial G} = (C_a - C_i) - G \cdot \frac{\partial C_i}{\partial G}. \quad \text{S1.3}$$

As A is a function of leaf photosynthetic capacity (V_{cmax} and J_{max}) and C_i, $f(V_{cmax}, J_{max}, C_i)$, $\partial A/\partial G$ also meets

$$\frac{\partial A}{\partial G} = \frac{\partial f}{\partial C_i} \cdot \frac{\partial C_i}{\partial G}. \quad \text{S1.4}$$

Equaling equation S1.3 and S1.4, we have:

$$(C_a - C_i) - G \cdot \frac{\partial C_i}{\partial G} = \frac{\partial f}{\partial C_i} \cdot \frac{\partial C_i}{\partial G}, \quad \text{S1.5}$$

and $\partial C_i/\partial G$ is

$$\frac{\partial C_i}{\partial G} = \frac{C_a - C_i}{\frac{\partial f}{\partial C_i} + G}. \quad \text{S1.6}$$

Applying equation S1.6 to equation S1.3 gives

$$\frac{\partial A}{\partial G} = (C_a - C_i) - G \cdot \frac{C_a - C_i}{\frac{\partial f}{\partial C_i} + G} = (C_a - C_i) \cdot \frac{\frac{\partial f}{\partial C_i}}{\frac{\partial f}{\partial C_i} + G}. \quad \text{S1.7}$$

As $\partial G/\partial E$ = 1 / (1.6 D), $\partial A/\partial E$ can be computed using

$$\frac{\partial A}{\partial E} = \frac{\partial A}{\partial G} \cdot \frac{\partial G}{\partial E} = \frac{C_a - C_i}{1.6 \cdot D} \cdot \frac{\frac{\partial f}{\partial C_i}}{\frac{\partial f}{\partial C_i} + G}. \quad \text{S1.8}$$

The limit of $\partial A/\partial E$ when E_{leaf} = 0 (namely G = 0) is $\frac{C_a - C_i}{1.6 \cdot D}$ (equation S1.2).

Notes S2 Derivation of the Manzoni model

The Manzoni model posits a plant maximizes the cumulative photosynthesis in a given amount of time plus an additional carbon gain by using the water remaining in the soil (Manzoni *et al.*, 2013):

$$\max\left(\int_0^{t_{\text{total}}} A \cdot \mathrm{d}t + \frac{1}{\Lambda} \cdot E_{\text{remain}}\right) \text{while } \int_0^{t_{\text{total}}} E_{\text{leaf}} \cdot \mathrm{d}t = E_{\text{total}} . \quad \text{S2.1}$$

The more the plant uses water during the time, the less water remains in the soil, and thus we have:

$$\mathrm{d}E_{\text{total}} = -\mathrm{d}E_{\text{remain}} . \quad \text{S2.2}$$

Further, according to the Cowan-Farquhar model, during the time, the marginal water use efficiency, i.e., $\partial A/\partial E = 1/\lambda$; and for an infinitesimal increase of $\mathrm{d}E_{\text{total}}$, the change of marginal water use efficiency is negligible. Therefore, at the optima of the Manzoni model, i.e.,

$$\frac{\mathrm{d}(\int A\mathrm{d}t)}{\mathrm{d}E_{\text{total}}} + \frac{\mathrm{d}(E_{\text{remain}}/\Lambda)}{\mathrm{d}E_{\text{total}}} = 0 , \quad \text{S2.3}$$

we have:

$$\frac{\mathrm{d}(\int A\mathrm{d}t)}{\mathrm{d}E_{\text{total}}} = \frac{1}{\lambda}, \quad \text{S2.4}$$

$$\frac{\mathrm{d}(E_{\text{remain}}/\Lambda)}{\mathrm{d}E_{\text{total}}} = -\frac{1}{\Lambda}, \quad \text{S2.5}$$

meaning the Manzoni model is optimized when $\lambda = \Lambda$.

The penalty and marginal penalty of the Manzoni model are defined as:

$$\Theta = \frac{E_{\text{leaf}}}{\Lambda}, \quad \text{S2.6}$$

$$\frac{\partial\Theta}{\partial E} = \frac{1}{\Lambda}. \quad \text{S2.7}$$

Notes S3 Derivation of the Prentice model

The Prentice model (Prentice *et al.*, 2014) also fits the general gain-penalty framework as the model can be written as:

$$\min\left(\frac{c_{\mathrm{E}}E_{\mathrm{leaf}}+c_{\mathrm{V}}V_{\mathrm{cmax}}}{A}\right)\equiv\max\left(\frac{A}{c_{\mathrm{E}}E_{\mathrm{leaf}}+c_{\mathrm{V}}V_{\mathrm{cmax}}}\right). \quad \text{S3.1}$$

Therefore, the penalty of the Prentice model is

$$\Theta = A\cdot\left(1-\frac{1}{\alpha\cdot(c_{\mathrm{E}}E_{\mathrm{leaf}}+c_{\mathrm{V}}V_{\mathrm{cmax}})}\right). \quad \text{S3.2}$$

Differentiating equation S3.2 gives:

$$\frac{\mathrm{d}\Theta}{\mathrm{d}E}=\frac{\mathrm{d}A}{\mathrm{d}E}\cdot\left(1-\frac{1}{\alpha\cdot(c_{\mathrm{E}}E_{\mathrm{leaf}}+c_{\mathrm{V}}V_{\mathrm{cmax}})}\right)+\frac{c_{\mathrm{E}}A}{\alpha\cdot(c_{\mathrm{E}}E_{\mathrm{leaf}}+c_{\mathrm{V}}V_{\mathrm{cmax}})^2}. \quad \text{S3.3}$$

However, there is a dA/dE term in the marginal penalty function. As the gain-penalty model is optimized when dA/dE = dΘ/dE, the Prentice model is optimized when

$$\frac{\mathrm{d}A}{\mathrm{d}E}=\frac{\mathrm{d}A}{\mathrm{d}E}\cdot\left(1-\frac{1}{\alpha\cdot(c_{\mathrm{E}}E_{\mathrm{leaf}}+c_{\mathrm{V}}V_{\mathrm{cmax}})}\right)+\frac{c_{\mathrm{E}}A}{\alpha\cdot(c_{\mathrm{E}}E_{\mathrm{leaf}}+c_{\mathrm{V}}V_{\mathrm{cmax}})^2}. \quad \text{S3.4}$$

Rearranging equation S3.4 gives:

$$\frac{\mathrm{d}A}{\mathrm{d}E}=\frac{c_{\mathrm{E}}A}{c_{\mathrm{E}}E_{\mathrm{leaf}}+c_{\mathrm{V}}V_{\mathrm{cmax}}}=\frac{A}{E_{\mathrm{leaf}}+\frac{c_{\mathrm{V}}}{c_{\mathrm{E}}}V_{\mathrm{cmax}}}. \quad \text{S3.5}$$

Therefore, the marginal risk function of the Prentice model is equivalent to

$$\frac{\mathrm{d}\Theta}{\mathrm{d}E}=\frac{A}{E_{\mathrm{leaf}}+\frac{c_{\mathrm{V}}}{c_{\mathrm{E}}}V_{\mathrm{cmax}}}. \quad \text{S3.6}$$

Notes S4 Mathematical considerations of the Lu model

The Lu model assumes a plant maximizes the mean photosynthetic rate weighted by the soil moisture distribution in a given amount of time. This assumption is equivalent to maximizing the total amount of the cumulative photosynthesis (Lu *et al.*, 2016). Thus, the Lu model is identical to the Cowan-Farquhar model.

The reason why the Lu model solution differed from the Cowan-Farquhar model is that mathematical errors were apparently made. For example, in their equation 12, the authors assumed

$$\frac{\mathrm{d}(\int z \cdot \mathrm{d}x)}{\mathrm{d}y} = \int \frac{\mathrm{d}z}{\mathrm{d}y} \cdot \mathrm{d}x \,, \qquad \text{S4.1}$$

which can be proven wrong by setting z = 1 and x = y (then $\frac{\mathrm{d}(\int z \cdot \mathrm{d}x)}{\mathrm{d}y}$ equals 1 but $\int \frac{\mathrm{d}z}{\mathrm{d}y} \cdot \mathrm{d}x$ equals 0). The correct equation should be:

$$\frac{\mathrm{d}(\int z \cdot \mathrm{d}x)}{\mathrm{d}y} = \frac{\mathrm{d}\left(\int z \cdot \frac{\mathrm{d}x}{\mathrm{d}y} \cdot \mathrm{d}y\right)}{\mathrm{d}y} = z \cdot \frac{\mathrm{d}x}{\mathrm{d}y}. \qquad \text{S4.2}$$

Notes S5 Mathematical and biological ambiguities in the Huang model

The Huang model assumes the stomata act to coordinate the leaf-xylem-phloem system to maximize sugar transport through the mesophyll cells to the phloem (Huang *et al.*, 2018). The difference between the Huang model and the Hölttä model is that the Huang model does not assume any negative feedback between sugar concentration and photosynthetic rate. From the physiological perspective, the Huang model can be written as:

$$\max\left(K_{\mathrm{xp}} \cdot S_{\mathrm{xp}} \cdot [P_{\mathrm{xy}} - P_{\mathrm{ph}}] \cdot \mathrm{SC}_{\mathrm{ph}}\right), \quad \text{S5.1}$$

where K_{xp} is the water permeability from xylem conduit to phloem, S_{xp} is the contact area between xylem conduit and phloem, P_{xy} is the water potential of the leaf xylem, P_{ph} is the water potential of the phloem cell, and $\mathrm{SC}_{\mathrm{ph}}$ is the sugar concentration in the phloem cell. Note here that leaf xylem water potential, P_{xy}, is different from leaf xylem pressure, P. In the xylem conduit, P_{xy} is the sum of water pressure (here it is P), osmotic water potential, and gravitational potential:

$$P_{\mathrm{xy}} = P - \mathrm{SC}_{\mathrm{xy}} RT + \rho g h\,, \quad \text{S5.2}$$

where $\mathrm{SC}_{\mathrm{xy}}$ is the solute concentration of xylem sap that is neglectable, RT is the gas constant times the Kelvin temperature, and h is the height of the xylem conduit. In the phloem conduit, P_{ph} is the sum of water pressure (here it is the turgor pressure of the phloem cell, $\mathrm{TP}_{\mathrm{ph}}$), osmotic water potential, and gravitational potential:

$$P_{\mathrm{ph}} = \mathrm{TP}_{\mathrm{ph}} - \mathrm{SC}_{\mathrm{ph}} RT + \rho g h\,, \quad \text{S5.3}$$

Combining equations S5.1–S5.3, the Huang model can be written as:

$$\max\left(K_{\mathrm{xp}} \cdot S_{\mathrm{xp}} \cdot [P - \mathrm{TP}_{\mathrm{ph}} + \mathrm{SC}_{\mathrm{ph}} RT] \cdot \mathrm{SC}_{\mathrm{ph}}\right) \quad \text{S5.4}$$

Equation S5.4 differs from their equations 10 and A.1 of Huang *et al.* (2018) because the authors made the following assumptions:

- phloem turgor pressure can be neglected;
- xylem water is the sole source of water into the phloem;
- xylem water pressure equals xylem water potential;
- all photosynthetic products are transported via the phloem.

The first assumption can only stand if the phloem sugar transport relies only on diffusion, which is not possible as more and more evidence suggests the transport is driven by Munch flow (e.g., Hölttä *et al.*, 2009; Rockwell *et al.*, 2018). The second assumption cannot stand because of the symplastic flow between the phloem cell and its companion cell. The third assumption results in

great error when *h* is unneglectable. The last assumption is not true because the sugars are also metabolized within the mesophyll cells.

Solving equation S5.4 requires modeling the carbon sink strength and computing the turgor pressure in the loading phloem cell, as the Hölttä model does. However, Huang *et al.* (2018) neglect the turgor pressure and further erroneously compute SC_{ph}. The unrealistic assumptions made by Huang *et al.* (2018) result in an incorrect interpretation of their model. The Huang model, if TP solved numerically, is the case of the Hölttä model that has no negative feedback from sugar concentration. The optimal solution of the Huang model, therefore, is max(*A*), and penalty and marginal penalty of Huang model are:

$$\Theta = 0, \qquad \text{S5.5}$$

$$\frac{\partial \Theta}{\partial E} = 0. \qquad \text{S5.6}$$

Therefore, the Huang model is a special case of the Cowan-Farquhar model (λ=0) and violates criteria C1 and C3–C7.

Notes S6 The Dewar MES model

The Dewar MES model assumes that mesophyll conductance (G_M) decreases as P gets more negative. This assumption holds correct if the more negative P results from drier soil because stomata also close more (Dewar *et al.*, 2018). However, if the more negative P results from more stomatal opening (i.e., when G increases), the assumption is not supported as G_M is reported to increase with G (Flexas *et al.*, 2013). Both the CAP and MES hypotheses that leaf photosynthetic capacity and G_M changes with the environment, like the sugar inhibition hypothesis made by the Hölttä model, hold promise for improving the modeling of photosynthesis, especially for long-term simulations. However, more investigations of whether and how the photosynthetic capacity and liquid-phase G_M change with the environment are required.

Figure S1

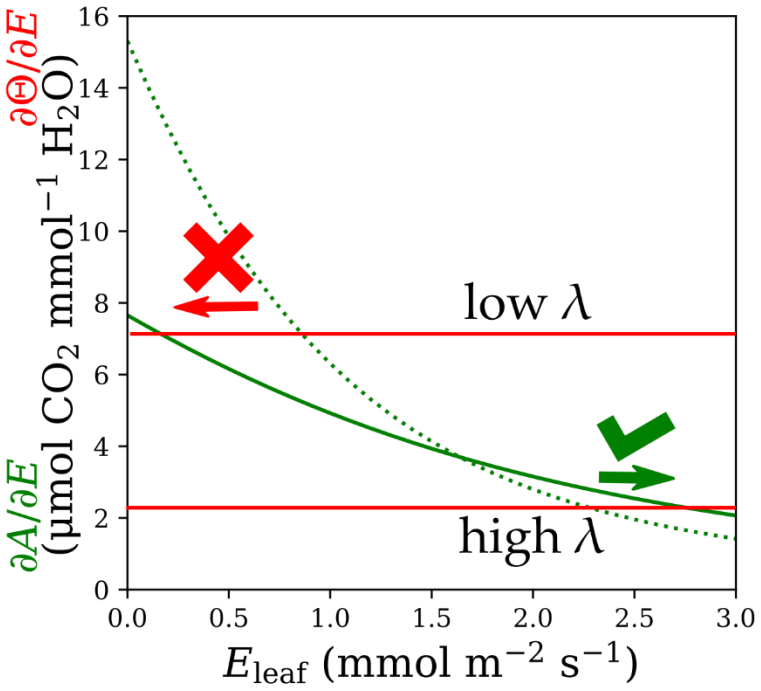

Figure S1 Explanations of why the Cowan-Farquhar model does not always predict realistic stomatal response to vapor pressure deficit (VPD). The green and red curves represent the marginal carbon again ($\partial A/\partial E$) and margian penalty ($\partial\Theta/\partial E$), respectively. The x-axis plots the increasing leaf transpiration rate (E_{leaf}) from left to right. The y-axis plots the $\partial A/\partial E$ and $\partial\Theta/\partial E$ with the unit μmol CO_2 $mmol^{-1}$ H_2O. When VPD increases, the margian carbon gain function shifts from the green dotted curve to the green solid curve. If the optimal $\partial\Theta/\partial E$ (namely $1/\lambda$ as in the main text) is low (namely λ is high), the Cowan-Farquhar model is able to predict realistic stomatal response to VPD (as indicated by the green arrow). However, if the optimal $\partial\Theta/\partial E$ is too high (namely λ is too low), the Cowan-Farquhar model fails to predict realistic stomatal response to VPD (as indicated by the red arrow). Though a constant λ can explain the apparent feedforward response, in this case the constant λ fails to predict the typical stomatal behavior. A constant λ cannot project the typical and apparent feedforward responses at the same time. Thus, it is better and physiologically more meaningful to attribute the apparent feedforward response to the potential changes of physiological traits rather than risking the predictive power of any model based on a constant λ.

Figure S2

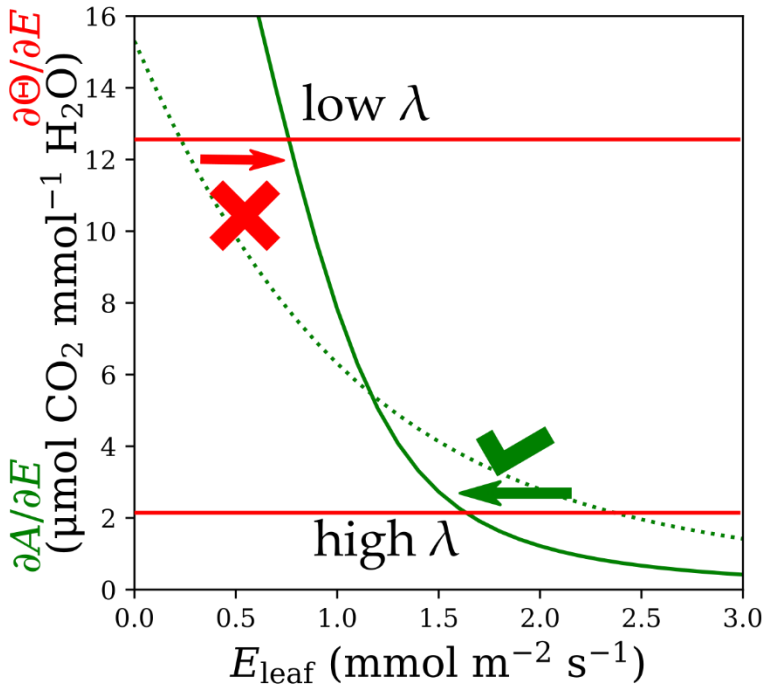

Figure S2 Explanations of why the Cowan-Farquhar model does not always predict realistic stomatal response to atmospheric [CO_2] (C_a). The green and red curves represent the marginal carbon again ($\partial A/\partial E$) and margian penalty ($\partial\Theta/\partial E$), respectively. The x-axis plots the increasing leaf transpiration rate (E_{leaf}) from left to right. The y-axis plots the $\partial A/\partial E$ and $\partial\Theta/\partial E$ with the unit μmol CO_2 $mmol^{-1}$ H_2O. When C_a increases, the margian carbon gain function shifts from the green dotted curve to the green solid curve. If the optimal $\partial\Theta/\partial E$ (namely $1/\lambda$ as in the main text) is low (namely λ is high), the Cowan-Farquhar model is able to predict realistic stomatal response to VPD (as indicated by the green arrow). However, if the optimal $\partial\Theta/\partial E$ is too high (namely λ is too low), the Cowan-Farquhar model fails to predict realistic stomatal response to C_a (as indicated by the red arrow).

Figure S3

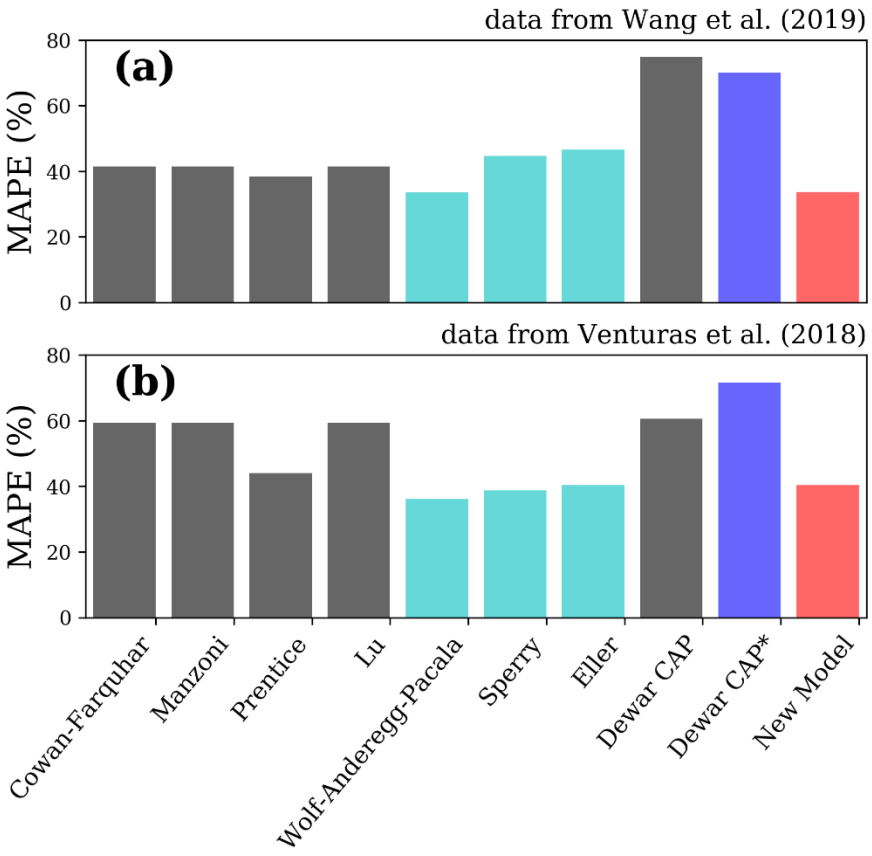

Figure S3 Model performance for birch and aspen datasets when rhizosphere conductance was set to infinity. **(a)** Data from water birch saplings exposed to changes in CO_2, atmospheric vapor pressure deficit (VPD), and soil moisture in a growth chamber (Wang *et al.*, 2019). **(b)** Data from aspen saplings exposed to natural changes in VPD and various levels of drought (Venturas *et al.*, 2018).

Table S1. Optimization model performance on three datasets. The MAPE stands for mean absolute percentage error (i.e., absolute error relative to the observed mean) for leaf photosynthetic rate (A), tree transpiration (E_{leaf}), and leaf xylem pressure (P). The Dewar CAP* model assumes the penalty is a "shadow cost" rather than a real decline in the instantaneous photosynthetic rate as in the original Dewar CAP version (Dewar *et al.*, 2018). For the birch and aspen datasets, the upper row for each model shows the MAPE with curve fitting the rhizosphere conductance, and the lower row for each model shows the MAPE by setting the rhizosphere infinity.

Model	**MAPE for birch (%)**				**MAPE for aspen (%)**				**MAPE for 36 sites (%)**
	A	***E*$_{leaf}$**	***P***	**mean**	***A***	***E*$_{leaf}$**	***P***	**mean**	**mean ± sd**
Cowan-Farquhar	44.3	52.7	26.3	41.1	42.0	56.5	33.2	43.9	111.2 ± 51.9
	45.9	52.9	25.6	41.4	78.4	57.2	42.6	59.4	
Manzoni	44.3	52.7	26.3	41.1	42.0	56.5	33.2	43.9	111.2 ± 51.9
	45.9	52.9	25.6	41.4	78.4	57.2	42.6	59.4	
Prentice	44.6	49.1	21.5	38.4	36.3	57.5	35.8	43.2	114.1 ± 62.5
	44.7	49.2	21.3	38.4	36.8	58.5	36.8	44.0	
Lu	44.3	52.7	26.3	41.1	42.0	56.5	33.2	43.9	111.2 ± 51.9
	45.9	52.9	25.6	41.4	78.4	57.2	42.6	59.4	
Wolf-Anderegg-Pacala	38.2	34.1	16.7	29.7	34.9	24.9	11.7	23.8	47.3 ± 14.0
	39.8	40.1	17.0	33.6	33.2	39.9	35.3	36.1	
Sperry	38.1	27.8	14.5	26.8	29.5	39.5	23.9	29.7	61.4 ± 38.8
	39.0	78.1	16.9	44.6	52.3	41.7	22.6	38.8	
Eller	38.3	31.4	16.8	28.8	25.7	36.8	24.5	29.0	60.9 ± 39.8
	40.8	81.2	17.7	46.6	56.9	42.1	22.2	40.4	
Dewar CAP	63.2	50.0	38.6	50.6	66.3	37.2	38.4	47.3	89.9 ± 39.6
	60.8	131.4	32.3	74.8	65.1	84.1	32.6	60.6	
Dewar CAP*	38.1	31.7	42.1	37.3	52.5	25.3	40.2	39.4	70.0 ± 37.5
	46.2	131.4	32.3	70.0	98.1	84.1	32.6	71.6	
New Model	37.4	34.2	12.7	28.1	25.1	37.7	24.8	29.2	52.9 ± 21.3
	37.9	50.6	12.6	33.7	54.7	42.8	23.3	40.3	

References

Dewar R, Mauranen A, Mäkelä A, Hölttä T, Medlyn BE, Vesala T. **2018**. New insights into the covariation of stomatal, mesophyll and hydraulic conductances from optimization models incorporating nonstomatal limitations to photosynthesis. *New Phytologist* **217**: 571–585.

Flexas J, Scoffoni C, Gago J, Sack L. **2013**. Leaf mesophyll conductance and leaf hydraulic conductance: An introduction to their measurement and coordination. *Journal of Experimental Botany* **64**: 3965–3981.

Hölttä T, Mencuccini M, Nikinmaa E. **2009**. Linking phloem function to structure: Analysis with a coupled xylem-phloem transport model. *Journal of Theoretical Biology* **259**: 325–337.

Huang C-W, Domec J-C, Palmroth S, Pockman WT, Litvak ME, Katul GG. **2018**. Transport in a coordinated soil-root-xylem-phloem leaf system. *Advances in Water Resources* **119**: 1–16.

Lu Y, Duursma RA, Medlyn BE. **2016**. Optimal stomatal behaviour under stochastic rainfall. *Journal of Theoretical Biology* **394**: 160–171.

Manzoni S, Vico G, Palmroth S, Porporato A, Katul G. **2013**. Optimization of stomatal conductance for maximum carbon gain under dynamic soil moisture. *Advances in Water Resources* **62**: 90–105.

Prentice IC, Dong N, Gleason SM, Maire V, Wright IJ. **2014**. Balancing the costs of carbon gain and water transport: Testing a new theoretical framework for plant functional ecology. *Ecology Letters* **17**: 82–91.

Rockwell FE, Gersony JT, Holbrook NM. **2018**. Where does Münch flow begin? Sucrose transport in the pre-phloem path. *Current Opinion in Plant Biology* **43**: 101–107.

Venturas MD, Sperry JS, Love DM, Frehner EH, Allred MG, Wang Y, Anderegg WRL. **2018**. A stomatal control model based on optimization of carbon gain versus hydraulic risk predicts aspen sapling responses to drought. *New Phytologist* **220**: 836–850.

Wang Y, Sperry JS, Venturas MD, Trugman AT, Love DM, Anderegg WRL. **2019**. The stomatal response to rising CO2 concentration and drought is predicted by a hydraulic trait-based optimization model. *Tree Physiology* **39**: 1416–1427.